Accepted Manuscript

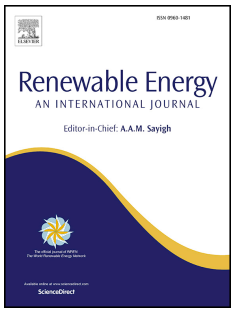

Application of extended vortex theory for blade element analysis of horizontal-axis wind turbines

D.H. Wood

PII: S0960-1481(17)31288-0

DOI: 10.1016/j.renene.2017.12.085

Reference: RENE 9582

To appear in: *Renewable Energy*

Received Date: 5 April 2017

Revised Date: 10 October 2017

Accepted Date: 24 December 2017

Please cite this article as: Wood DH, Application of extended vortex theory for blade element analysis of horizontal-axis wind turbines, *Renewable Energy* (2018), doi: 10.1016/j.renene.2017.12.085.

Application of Extended Vortex Theory for Blade Element Analysis of Horizontal-axis Wind Turbines

D.H.Wood

Department of Mechanical and Manufacturing Engineering, University of Calgary, Calgary T2N 1N4, AB, Canada. E-mail: dhwood@ucalgary.ca

Abstract

Vortex theory is used in blade element analysis (BEA) of wind turbines to account for the finite number of blades, N, usually in terms of Prandtl's "tip loss function", F. Wood et al. [1] calculated alternative "trailing vorticity functions" using helical vortex theory. F was found to be inaccurate over the entire blade at low tip speed ratio and in error near the hub at any tip speed ratio. Further, the trailing vorticity function is not constrained to be less than unity as is F. Wood & Okulov [2] analyzed the nonlinear terms in the streamtube equations for angular and axial momentum and found an accurate way of including these in BEA. This paper describes the use of the trailing vorticity functions, which can be different in the axial and azimuthal directions, in an otherwise standard blade element analyses. Comparison is made to wind tunnel tests of model rotors and to calculations using F. There is only a small difference in the calculated power and thrust coefficients. The present calculations show higher induced axial velocities in the tip and hub regions and it is suggested that the trailing vorticity functions can be used in situations where F cannot.

Key words: wind turbine, tip loss, blade element analysis, trailing vorticity function

1. Introduction

Blade element analysis (BEA) is, and will remain, an important part of wind turbine aerodynamics. van Kuik et al. [1] make the following statement

about the future research agenda for wind energy: "In parallel to the reduction in cost of computational fluid dynamics (CFD), improving the accuracy of simplified models [such as BEA] is one of the key scientific and engineering challenges for wind energy." The basis for optimism about BEA is its combination of accuracy and simplicity. It is the method of choice for preliminary wind turbine blade design which often uses multi-dimensional optimization, e.g. Sessarego et al. [2]. BEA executes quickly in comparison to high fidelity computational fluid dynamics simulations, and so allows easier and faster exploration of the multi-parameter design space.

BEA assumes that a blade is comprised of elements which obey the Kutta-Joukowsky (KJ) theorem, Okulov et al. [3]. The KJ forces on each element are then iteratively balanced against the change in axial and angular momentum in the flow over the element to determine the torque, power, and thrust. Different modifications have been made to to BEA to account for high thrust, stall delay, and finite blade number, N, e.g Burton et al. [4]. This paper is concerned with the last for the very practical reasons that most turbines have $N = 3$, and the inclusion of the effects of finite N is a subject where the theory of helical vortices can make important contributions.

The traditional modification to BEA for finite N is through the "tip loss factor" in the form originally derived by Prandtl and implemented by Glauert, denoted F_P, see Section 3.8.2 of Burton et al. [4]. Prandtl's original derivation is not easily found but Glauert [5] and Sørensen [6] derive F_P by approximating the helicoidal trailing vorticity as two-dimensional sheets. It is

generally held that F_P is inaccurate at low values of the tip speed ratio, λ, but becomes accurate at values typical of modern wind turbine operation, $\lambda \approx 7$. Tip loss is also incorporated in the streamtube equations for momenutm and angular momentum in various ways, as discussed by Wilson & Lissaman [7], de Vries [8], Shen et al. [9], and Clifton-Smith [10]. Schmitz & Maniaci [11] used a free vortex wake model with BEA to develop an alternative to Prandtl's F_p. Their method automatically accounts for wake expansion and vortex rollup but does not provide a general analytic formulation that can be absorbed into a BEA code. Wimhurst & Willden [12] further developed the tip correction method of Shen et al. [9] and found that corrections differed between axial and tangential components with the latter being larger. Again, no general correction was developed.

Wood et al. [13] pointed out that the lifting line assumption inherent in BEA makes finite-N effects entirely dependent on the trailing vorticity when the blades are straight and so a better name for it would be "trailing vorticity function" symbolized by F. They calculated F from helical vortex theory which was pioneered by Kawada [14], [15], and Hardin [16]. A summary of the history, including the rediscovery of Kawada's contributions, can be found in Fukumoto et al. [17]. The Kawada-Hardin equations give the velocity field external to a singly-infinite vortex of pitch p and constant radius t. p is defined such that a complete revolution of the helix occurs over a streamwise distance of $2\pi p$. For example, the circumferential velocity at a point aligned

with the start of the vortex whose radius, r, satisfies $r < t$, is

$$w(r,\theta) = \frac{N\Gamma t}{4\pi pr}\sum_{1}^{\infty} mK'_m(mt/p)I_m(mr/p)cos(m\theta) \tag{1}$$

where $K(.)$ and $I(.)$ are modified Bessel functions in standard notation and the differentiation is with respect to the argument. Γ is the vortex strength. Okulov [18] developed approximations to Equation (1) and those for the other components, which reduce significantly the computational time needed for their evaluation. These approximations were shown by Wood et al. [13] to give very accurate estimates for F for the Betz-Goldstein (BG) class of ideal rotors which are characterized by constant p across the wake. Summing the equations for N blades leads to a significant simplification that Wood et al. [13] called "Kawada cancellation": terms containing $cos(m\theta)$ are non-zero only when m is an integer multiple of N, so that 2/3rds of them drop out for a three-bladed rotor. The main aim of this paper is to explore the application of these recent extensions of helical vortex theory to BEA.

The analysis of BG rotors produced another, unexpected benefit. Wood & Okulov [19] proved very simply that Glauert's intuitive incorporation of F in the streamtube equations is exact for BG rotors. The equation for the thrust coefficient, C_T, is

$$\frac{dC_T}{dr} = 8a(1-a_b)r = 8a_bF_u(1-a_b)r \tag{2}$$

and for the torque coefficient, C_Q, is

$$\frac{dC_Q}{dr} = 8a'\lambda r(1-a_b)r^2 = 8a'_b F_w \lambda(1-a_b)r^3, \tag{3}$$

where r is the radius of the blade element, a is the streamtube-average axial induction factor, a_b is the value at the blades, and a' and a'_b are the corresponding rotational induction factors[1]. Another difference from the simple Prandtl approximation is evident in Equations (2) and (3): F for the axial flow, F_u, is not necessarily equal to F_w for the circumferential motion. This difference was anticipated by Shen et al. [9] but not investigated by them. Wimhurst & Willden [12] appear to be the first to consider the difference. It is easy to show that $F_u = F_w$ only for BG rotors, so the inequality between F_u and F_w has to be maintained for generality.

$1 - a_b$ appearing on the right side of Equations (2) and (3)can be interpreted as an approximate inclusion of nonlinear effects in the streamtube equations for axial and angular momentum. These equations are usually derived using the streamtube-average values of axial, $1 - a$, and circumferential velocity, $a'\lambda r$. Wood & Okulov [19] pointed out, however, that both the axial and angular momentum equations are nonlinear and the correlated departures from the means cause "nonlinear" or "quadratic" terms in their Equation (11) for example. The nonlinear terms can exceed 10% of the con-

[1]The version of Equation (3) in Wood & Okulov [19] - their Equation (6) - should be multiplied by λr on the right hand side.

ventional terms for C_Q for $N = 3$ when $\lambda \approx 1$ and F deviates significantly from unity. Equations (2) and (3) both account for the nonlinearity, but only approximately because the nonlinear terms are dominated by the interaction of blade and wake components, Wood & Okulov [19], whereas, it was pointed out above that F_u and F_w are caused entirely by the wake. Since there does not appear to be any simple improvement, Equations (2) and (3) will be used in the present analysis.

The ultimate aim of the work described in this paper is to applications of BET where Prandtl's tip loss cannot or should not be used. These cases include coned rotors, as mentioned above, where F_u and F_w are still entirely determined by the trailing vorticity if the blades remain straight. If they bend, then the bound vorticity influences F_u and F_w, as it must for rotors with blades of unequal aerodynamic loading as would occur if blades had individual pitch adjustment, Wood [20]. If a blade has a flap or discontinuity in pitch or chord, the model developed here should naturally account for the rapid changes in bound circulation. The diffuser shrouding a diffuser-augmented wind turbine induces a circumferentially-uniform axial flow but does not directly effect the azimuthal motion, so F_u may be significantly different from F_w. Finally, unsteadiness in pitch angle, wind speed or yaw, causes time dependence of the shed vorticity, and, very likely, large changes in the the effect of that vorticity on the blade elements. It seems reasonable to begin this work with the simplest and best documented case of steady flow through unconed blades without a diffuser.

The remainder of the paper contains, in the next Section, a description of the basic features of BEA and the calculation of F_u and F_w. The following section describes the two wind tunnel experiments on two- and three-bladed rotors that are used for comparison to conventional BEA and the modifications proposed here. The remaining discussion and all conclusions are given in the last section.

2. Determination of F and Blade Element Analysis

From the KJ theorem, Okulov & Sørensen [21] gave the equations for thrust, T, and torque, Q, as a function of blade radius, r:

$$\frac{dT}{dr} = \rho N \Gamma \lambda (1 + a'_b) r \tag{4}$$

and

$$\frac{dQ}{dr} = \rho N \Gamma (1 - a_b) r \tag{5}$$

where ρ is the density and Γ is now the bound circulation of the element at radius r. All lengths are normalized by the rotor radius, and axial velocities by the wind speed. $a'_b = w_{wb}/(\lambda r) + a'$ where w_{wb} is the departure from the streamtube-average circumferential velocity at the blade due to the trailing vorticity in the wake, hence the additional subscript "w". w_{wb} for BG rotors from Okulov's [18] approximation is given by Equation (19) of [13]. From the same approximation, u_{wb}, the departure from the streamtube-average for

the axial motion, is, for the general case of varying p,

$$u_{wb}(r) \sim \frac{1}{4\pi}\int_0^r \frac{\partial\Gamma}{\partial t}\left[\frac{p^2(t)+t^2}{p^2(t)+r^2}\right]^{1/4} \left[\frac{-N}{p(t)(1-e^{\xi N})}+\frac{1}{24}\left(\frac{2p^2(t)+9t^2}{(p^2(t)+t^2)^{3/2}}-\frac{2p^2(t)-3r^2}{(p^2(t)+r^2)^{3/2}}\right)\log(1-e^{-\xi N})\right]dt + \frac{1}{4\pi}\int_r^1 \frac{\partial\Gamma}{\partial t}\left[\frac{p^2(t)+t^2}{p^2(t)+r^2}\right]^{1/4} \left[\frac{N}{p(t)(1-e^{-\xi N})}+\frac{1}{24}\left(\frac{2p^2(t)+9t^2}{(p^2(t)+t^2)^{3/2}}-\frac{2p^2(t)-3r^2}{(p^2(t)+r^2)^{3/2}}\right)\log(1-e^{\xi N})\right]dt \tag{6}$$

where

$$e^{\xi} = \frac{r\left[p(t)+\sqrt{p^2(t)+t^2}\,\right]exp\sqrt{1+r^2/p^2(t)}}{t\left[p(t)+\sqrt{p^2(t)+r^2}\,\right]exp\sqrt{1+t^2/p^2(t)}}. \tag{7}$$

The general equation for $w_{wb}(r)$ is obtained by multiplying the integrands in (6) by $p(t)/r$. Thus little extra time is used in computing F_w as well as F_u. As explained by Wood & Okulov [19], Kawada cancellation has been used to simplify Equation (6) which was evaluated for r at the centre of each element over which Γ is constant. Thus the contributions to the integrals in Equation (6) come from the vortices trailing from the element junctions. The first integral in Equation (6)was replaced by the sum of the product of the terms multiplying $\partial\Gamma/\partial t$ and the increment in Γ over all element junctions below the element at r. In those terms, t becomes the radius of vortex shed at the element junctions with a strength equal to the increment in Γ. Then,

the second integral was similarly approximated for all junctions above the element at r. The determination of the vortex pitch, p will be described below. It follows that

$$F_u = a/(a + u_{wb}) \tag{8}$$

and

$$F_w = a'/\big(a' + w_{wb}/(\lambda r)\big) \tag{9}$$

The current implementation of BEA is a development of the program described in Chapter 6 of Wood [22] which was closely based on Shen et al. [9], with two main differences: the function g defined by Equations (25) and (26) in Shen et al. [9] was not implemented, so that F_P was found using $g = 1$. Second, instead of Equations (2) and (3) they used

$$\frac{dC_T}{dr} = 8a_b F_p(1 - a_b F_p)r \tag{10}$$

and

$$\frac{dC_Q}{dr} = 8a'_b F_p \lambda(1 - a_b F_p)r^3. \tag{11}$$

Shen et al. [9] defined

$$Y_1 = 4F \sin^2 \phi/(\sigma C_a) \tag{12}$$

where ϕ is the usual inflow angle in the blade element velocity triangle, defined, for example, in Fig. 3.14 of Burton et al. [4] and Figure 3.2 of Wood [22]. $\sigma = Nc/(2\pi r)$, where c is the element chord, is the local solidity and

C_a is the axial component (in coefficient form) of the resultant force on the blade element. Similarly,

$$Y_2 = 4F \sin\phi \cos\phi/(\sigma C_{a'}) \tag{13}$$

where $C_{a'}$ is the tangential component of the total force. By equating the streamtube equations (10) and (11) to the element forces, Shen et al. [9] obtained their Equations (28) and (29) for the iterative solution of a and a'. For the present implementation of BEA using F_u and F_w as examples:

$$Y_1' = 4F_u \sin^2\phi/(\sigma C_a) \tag{14}$$

and

$$Y_2' = 4F_w \sin\phi \cos\phi/(\sigma C_{a'}) \tag{15}$$

for which Equation (2) gives

$$a_b = 1/(Y_1' + 1) \tag{16}$$

and Equation (3) gives

$$a_b' = 1/(Y_2' - 1) \tag{17}$$

showing that both F_u and F_w are needed to solve iteratively Equations (16) and (17). It remains to specify the blade element p and Γ which are needed to determine F_u and F_w using Equations (6) and (7). There appear to be

two possible implementations of the present helix model: either each blade element or each junction has a unique p. The former requires more computation as it allows the vorticity shed from adjacent elements to have different trajectories but is conceptually easier. It implies that the mean velocities for each element at the rotor are determined entirely by the helices shed by the element. This gives

$$a = a_b F_u = N\Gamma/(4\pi p) \tag{18}$$

and

$$\lambda r a' = \lambda r a'_b F_w = N\Gamma/(4\pi r) \tag{19}$$

which holds for either implementation. Equation (18) allows the use of Wood & Okulov's [19] result that

$$p = dC_Q/dC_T. \tag{20}$$

However, it was found necessary to calculate the pitch directly from (18). For consistency with (19), Γ is determined from

$$\Gamma = \frac{1}{2} U_T C_l \big(1 - \frac{C_d}{C_l \tan\phi}\big) \tag{21}$$

where U_T is the total blade element velocity, C_l and C_d are the element lift and drag coefficients, respectively. Equations (18-21) give two equations for each of the pitch and circulation which will be compared to check the consistency of the iterated solutions to the blade element equations.

The use of vortex theory does not, unfortunately, account for high thrust and the need for correction of the equation for dC_T/dr in this region. By analogy with Equation (30) of Shen et al. [9], Equation (2) was modified whenever $a_b > a_c = 1/3$ to read

$$dC_T/dr = 8[a_c^2 + (1 - 2a_c)a_b]F_u r \tag{22}$$

from which

$$a_b = 1 + Y_1'(\frac{1}{2} - a_c^2) - \frac{\sqrt{Y_1'}}{2}\sqrt{4 + Y_1' + 4a_c(a_c - 2 - Y_1'(1 - a_c))} \tag{23}$$

with no change to Equation (17) for a_b'. For comparison with the measurements described in the next two Sections, "conventional BEA" refers to the determination of a_b and a_b' from Equations (16) and (17) with F_u and F_w respectively replaced by F_P given by Equation (3.81) of Burton et al. [4] which combines "tip" and "hub" losses. The "modified" BEA uses Equations (16) and (17) with F_u and F_w calculated as explained above. The analyses use the same airfoil data which has not been corrected for solidity and/or rotational effects. In other words, the only difference between the calculations is in the choice of F.

3. The Simulated Wind Turbines

Comparison of the conventional and modified BEA was was made to two wind tunnel experiments: the two-bladed rotor of Anderson et al. [23] and

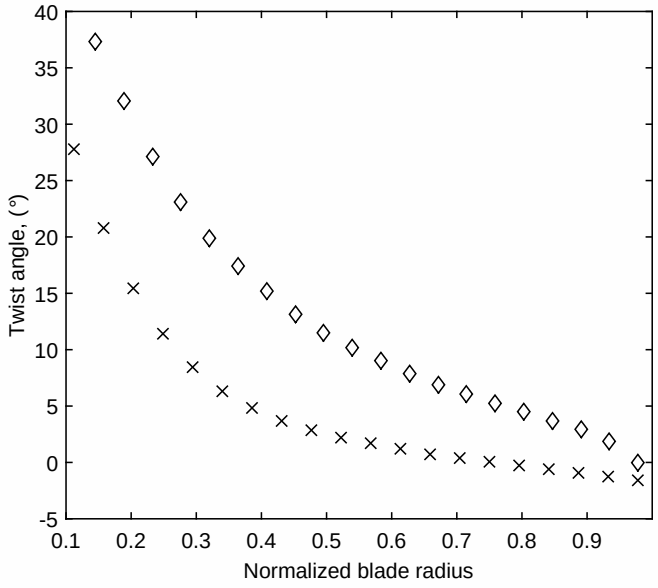

Figure 1: Twist distribution of simulated blades from Anderson et al. [23], solid line; from Krogstad & Eriksen [24], ◊.

the three-bladed one of Krogstad & Eriksen [24]. The chord distribution of the blades is shown in Figure 1 and the twist in Figure 2. Anderson's turbine had a radius of 1.5 m and was tested at 10 m/s in a wind tunnel where the rotor area was 12% of the working section cross-section. "Small" blockage corrections were made to the power coefficient, C_P, and the thrust coefficient, C_T. The lift and drag coefficients for the NACA 4412 section used by Anderson et al. [23] were taken from Miley [25] and are shown in Figure 5.1 of Wood [22] where the experiment of [23] was discussed extensviely to provide the context of BEA. This experiment was also considered at length by R.E. Wilson in Chapter 5 of Spera [26]. The lift and drag data is limited to angles of attack, $\alpha < 12°$, which means that the simulations were limited

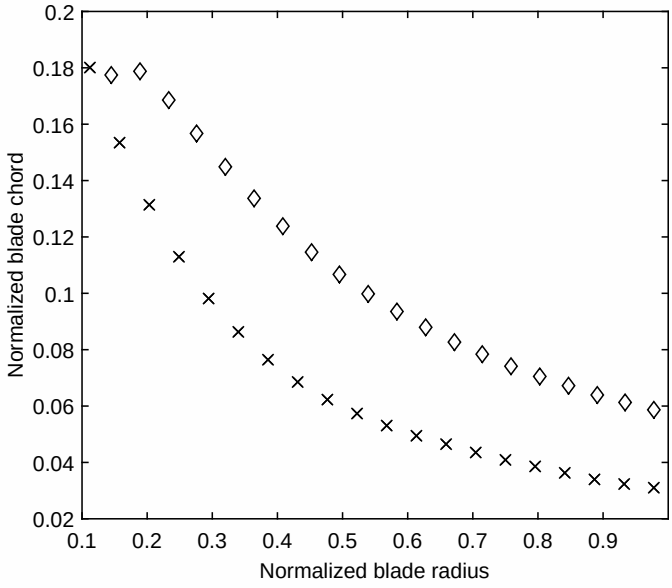

Figure 2: Chord distribution of simulated blades from Anderson et al. [23], solid line; from Krogstad & Eriksen [24], ◊.

to $\lambda \geq 7$.

The 0.447 m radius, three-bladed rotor of Krogstad & Eriksen [24] was tested in a tunnel with a $2m \times 3m$ cross-section giving a very similar blockage to that of Anderson's experiments. No blockage corrections were made. Krogstad & Eriksen [24] state that C_P and C_T were independent of Re when the wind speed exceeded 9 m/s so the present simulations were done for 10 m/s. The blades used the S826 airfoil for which lift and drag data for angle of attack, α, between $-16.5°$ and 29° and Reynolds number Re, $70,000 \leq Re \leq 100,000$ were provided by J. Bartl, see Sagmo et al. [27]. This restriction on Re meant that the simulations were restricted to $\lambda \geq 4$.

Table 1: Variation of Power and Thrust for BET with Number of Blade Elements for $\lambda = 10$, Anderson et. al [23]

No. Elements	C_P **for** F_P	C_T **for** F_P	C_P **for** F_u, F_w	C_T **for** F_u, F_w
10	0.460	0.810	0.468	0.815
20	0.456	0.808	0.460	0.811
40	0.454	0.808	0.454	0.808
60	0.453	0.807	0.453	0.806

4. Blade Element Calculations

The blades were divided into equispaced blade elements ranging from the hub to the tip. Table 1 shows the variation in power and thrust with number of elements for the experiment of Anderson et al. [23]. All subsequent calculations in this paper used 40 elements.

The implementation of the new method began with $F_u = F_w = 1$. The blade element calculations were then iterated for all elements to within a relative convergence of 10^{-5} before the trailing vorticity calculations of F_u and F_w using Γ from Equation (21) and p from (18). The calculations were stopped at the λ where the outer 50% of the blade was in the high thrust region. The same relative tolerance was used for the conventional BEA calculations.

The predicted C_P and C_T from conventional and modified BEA for Anderson's experiment are compared to the measurements in Figures 3 and 4 respectively along with the results for no correction, i.e. with $F_P = F_u = F_w = 1$. The Prandtl and vortex theory corrections reduce the power by around 10% and clearly increase the accuracy of the BEA calculations but

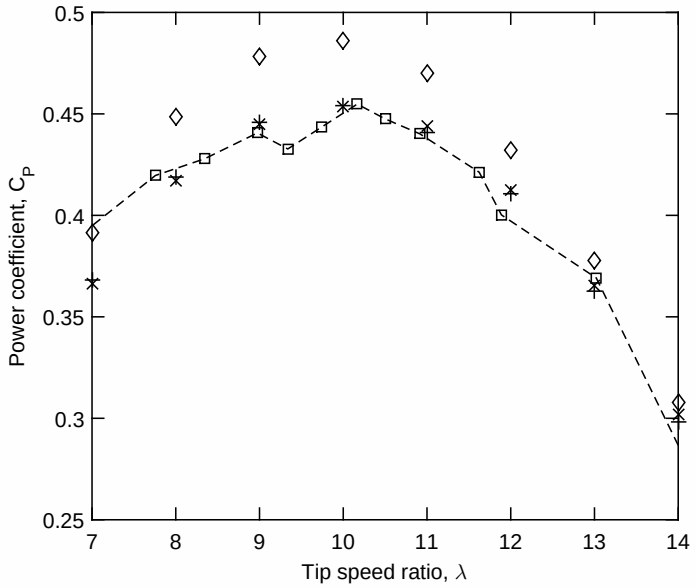

Figure 3: Calculated power coefficient compared to the measurements of Anderson et al. [23], □. ◊, BEA with $F_p = F_u = F_w = 1$;×, modified BEA; +, conventional BEA.

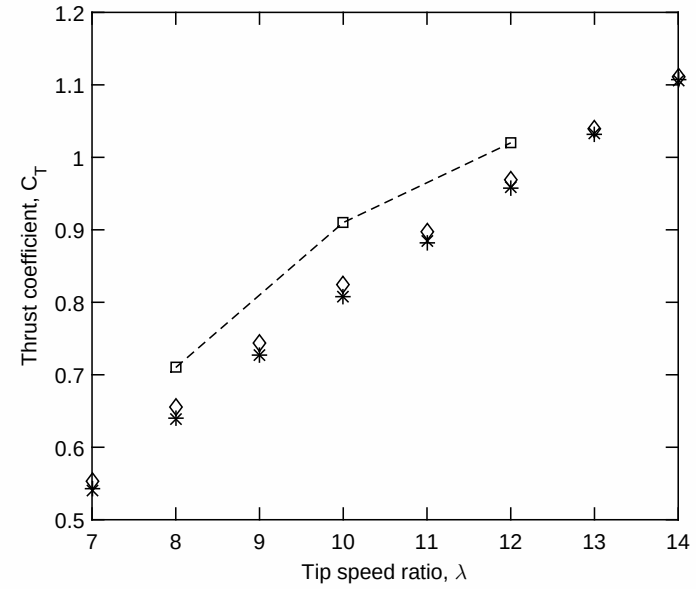

Figure 4: Calculated thrust coefficient compared to the measurements of Anderson et al. [23], □. ◊, BEA with $F_p = F_u = F_w = 1$; ×, modified BEA; +, conventional BEA.

have only a small effect on the thrust. There is very little difference in the predictions using F_P and F_u and F_w of these integral performance parameters at all λ. The same general behaviour occurs for the three-bladed rotor as well, Figures 5 and 6. For both turbines the differences between the conventional and modified power reduce as λ increases and $F_P, F_u, F_w \to 1$ over the whole blade as finite blade effects reduce.

As examples of the distribution of forces and flow along the blades, the blade element torque for the two-bladed rotor at $\lambda = 7$ is shown in Figure 7, plotted such that λ times the sum of the torques equals C_P. The agreement of the global parameters C_P and C_T is reflected in the agreement of the elemental torque. F_P, F_u, and F_w are shown in Figure 8 for the two-bladed rotor at $\lambda = 7$. It is not clear whether the local maxima in F_u and F_w near $r/R = 0.4$ are genuine: as pointed out by Wood et al. [13] and Okulov & Wood [19] neither F_u nor F_w is constrained to be less than unity as is F_P, but it has been noticed that the smoothness of the distributions appears to be influenced by the smoothness of the lift and drag data. The substantial differences between F_u and F_w and between these and F_P are not reflected in the blade element torque. The two determinations of F_u and, separately, of F_w are in good agreement except near the blade tip where F_w appears incorrect, The effect of this is likely to be small, however, as $a'F_w$ varies smoothly and is small near the tip as shown in Figure 9.

Figure (9) also shows the calculated bound circulation and vortex pitch for $\lambda = 7$. The two separate merthods of determining both these quantities give

closely matched results, suggesting that the BEA iterations have converged sufficiently. Both Γ and p are reasonably uniform, with the latter result being the explanation for the closeness of F_u and F_w in Figure 8. The major difference between the two methods of determining F is shown in the axial induction factor results in Figure 10 for the two-bladed rotor at $\lambda = 7$. The new method gives lower F_u and therefore higher a both near the hub and near the tip.

5. Summary and Conclusion

This paper considers two contributions of modern vortex theory to the blade element analysis of horizontal-axis wind turbines. The first is the formulation of the trailing vorticity functions which account, among other things, for the finite number of blades. These functions, or their extensions, should be more general than the commonly-used Prandtl tip loss.

The second contribution is the testing of the finding by Wood & Okulov [19] that Glauert's intuitive correction for finite blade number effects in the streamtube axial and angular momentum equations is exact for the restricted class of Betz-Goldstein rotors where the vortex pitch is constant across the wake. Glauert's corrections account approximately for the nonlinear velocity terms in the streamtube equations. The trailing vorticity functions and Glauert's corrections were included in an otherwise conventional blade element analysis that was compared to wind tunnel tests of two- and three-bladed model wind turbines and to calculations using the conven-

tional Prandtl tip loss. These experiments provide a more general test of vortex theory because the pitch varies across the wake. Surprisingly, the new formulations do not lead to improved predictions of rotor power and thrust, even at low tip speed ratio where the traditional approximation of Prandtl is known to be inaccurate. Despite significant differences between the trailing vorticity functions and Prandtl's tip loss, the largest difference in the other quantities of importance was to the axial induction factor. The modified BEA gave higher values near the tip and hub.

6. Acknowledgments

This work was supported by the NSERC Discovery Grant Scheme, the NSERC Industrial Research Chairs program and the ENMAX Corporation. Professor Per-Åge Krogstad, NTNU, generously provided experimental data from his model wind turbine and Jan Bartl, NTNU, sent me the lift and drag data of the S826 airfoil. I also value the advice of Professor Gijs van Kuik, TU Delft, on matters related to wind turbine blades and flaps.

7. References

[1] G. A. M. van Kuik, J. Peinke, R. Nijssen, D. Lekou, J. Mann, J. N. Sørensen, C. Ferreira, J. W. van Wingerden, D. Schlipf, P. Gebraad, H. Polinder, A. Abrahamsen, G. J. W. van Bussel, J. D. Sørensen, P. Tavner, C. L. Bottasso, M. Muskulus, D. Matha, H. J. Lindeboom, S. Degraer, O. Kramer, S. Lehnhoff, M. Sonnenschein, P. E. Sørensen,

R. W. Knneke, P. E. Morthorst, and K. Skytte, "Long-term research challenges in wind energy – a research agenda by the european academy of wind energy," Wind Energy Science, vol. 1, pp. 1–39, feb 2016.

[2] M. Sessarego, K. Dixon, D. Rival, and D. Wood, "A hybrid multi-objective evolutionary algorithm for wind-turbine blade optimization," Engineering Optimization, vol. 47, pp. 1043–1062, aug 2015.

[3] V. L. Okulov, J. N. Sørensen, and D. H. Wood, "Rotor theories by Professor Joukowsky: Vortex theories," Progress in Aerospace Sciences, vol. 55, pp. 19–46, 2015.

[4] T. Burton, N. Jenkins, D. Sharpe, and E. Bossanyi, Wind Energy Handbook. John Wiley & Sons, 2nd Edn, 2011.

[5] H. Glauert, Division L, Airplane Propellers, in Aerodynamic Theory, ch. XI. Springer, 1935.

[6] J. N. Sørensen, General Momentum Theory for Horizontal Axis Wind Turbines. Springer, 2016.

[7] R. E. Wilson and P. B. S. Lissaman, "Applied aerodynamics of wind power machines," tech. rep., Oregon State University, 1974.

[8] O. de Vries, "Fluid dynamic aspects of wind energy conversion," tech. rep., AGARDograph No. 243, 1979.

[9] W. Z. Shen, R. Mikkelsen, J. N. Sørensen, and C. Bak, "Tip vortex corrections for wind turbine computations," Wind Energy, vol. 8, pp. 457–475, 2005.

[10] M. J. Clifton-Smith, "Wind turbine blade optimization with tip loss corrections," Wind Engineering, vol. 35, pp. 477–406, 2009.

[11] S. Schmitz and D. C. Maniaci, "Methodology to determine a tip-loss factor for highly loaded wind turbines," AIAA Journal, vol. 55, pp. 341–351, 2017.

[12] A. Wimhurst and R. H. J. Willden, "Analysis of a tip correction factor for horizontal axis turbines," vol. 20, pp. 1515–1528, 2017.

[13] D. H. Wood, V. L. Okulov, and D. Bhattacharjee, "Direct calculation of wind turbine tip loss," Renewable Energy, vol. 95, pp. 269–276, 2016.

[14] S. Kawada, "Induced velocity by helical vortices," Journal of Aeronautical Sciences, vol. 36, no. 3, pp. 86–87, 1936.

[15] S. Kawada, "Calculation of induced velocity by helical vortices and its application to propeller theory," Tech. Rep. 172, Aeronautical Research Institute, Tokyo Imperial University, 1939. http://repository.tksc.jaxa.jp/pl/dr/IS4146951000/en.

[16] J. C. Hardin, "The velocity field induced by a helical vortex filament," Physics of Fluids, vol. 25, pp. 1949–1952, 1982.

[17] Y. Fukumuto, V. L. Okulov, and D. H. Wood, "The contribution by Kawada to the analysis of the velocity induced by a helical vortex filament," Applied Mechanics Reviews, vol. 67, pp. 060801–1–7, 2015.

[18] V. Okulov, "On the stability of multiple helical vortices," Journal of Fluid Mechanics, vol. 521, pp. 319–342, 2004.

[19] D. Wood and V. Okulov, "Nonlinear blade element-momentum analysis of Betz-Goldstein rotors," Renewable Energy, vol. 107, pp. 542–549, jul 2017.

[20] D. Wood, "A cascade model of blade element interaction for wind turbines with unequal blades," International Journal of Sustainable Energy, vol. 35, no. 5, pp. 502–512, 2016.

[21] V. L. Okulov and J. N. Sørensen, "Refined Betz limit for rotors with a finite number of blades," Wind Energy, vol. 11, pp. 415–426, 2008.

[22] D. Wood, Small Wind Turbines: Analysis, Design, and Application. Springer, 2011.

[23] M. Anderson, D. Milborrow, and R. J.N., "Performance and wake measurements on a 3 m diameter horizontal axis wind turbine," in 4th Int. Symp. Wind Energy Systems, pp. 113–132, 1982.

[24] P. Å. Krogstad and P. E. Eriksen, ""blind test calculations of the performance and wake development for a model wind turbine," Renewable Energy, vol. 50, pp. 325–333, feb 2013.

[25] S. Miley, "A catalog of low Reynolds number airfoil data for wind turbine applications.," tech. rep., U.S. DoE Wind Energy Program, 1982.

[26] D. Spera, Wind Turbine Technology. ASME Publishing, 1994.

[27] K. F. Sagmo, J. Bartl, and L. Stran, "Numerical simulations of the nrel s826 airfoil.," Journal of Physics: Conference Series, vol. 753, p. 082036, sep 2016.

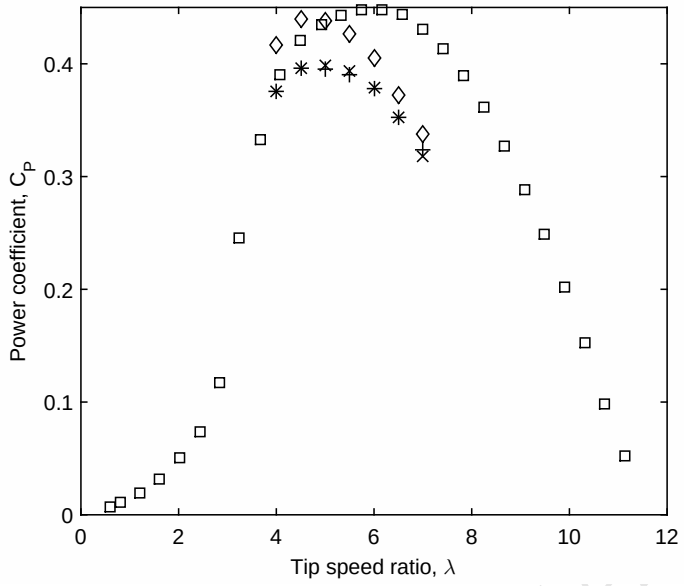

Figure 5: Calculated power coefficient compared to the measurements of Krogstad & Eriksen [24]. ♢, BEA with $F_p = F_u = F_w = 1$; □. +, modified BEA; ×, conventional BEA.

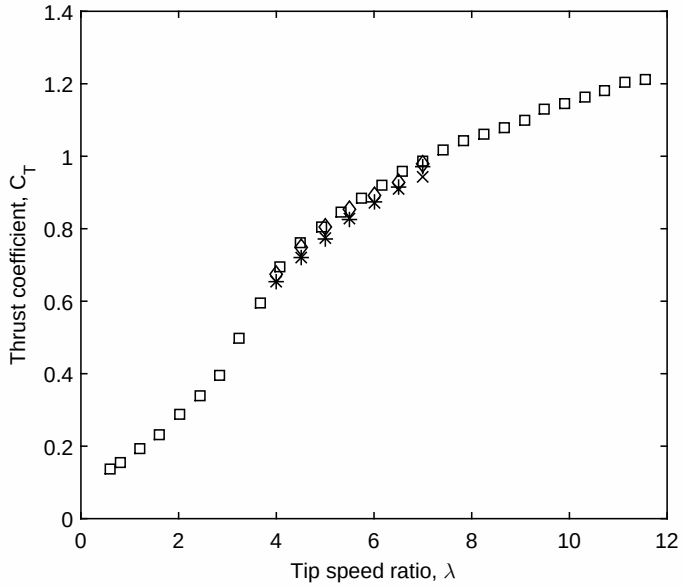

Figure 6: Calculated thrust coefficient compared to the measurements of Krogstad & Eriksen [24]. ♢, BEA with $F_p = F_u = F_w = 1$; □. +, modified BEA; ×, conventional BEA.

+

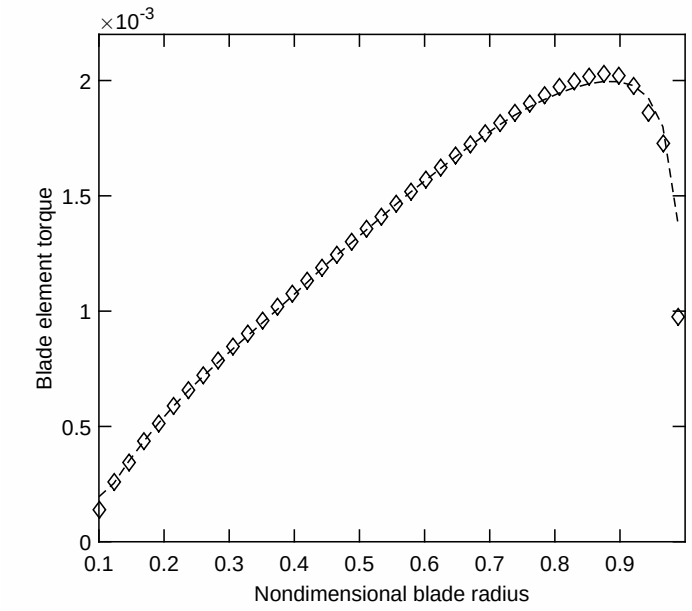

Figure 7: Calculated blade element torque for experiment of of Anderson et al. [23], $\lambda = 7$. $\Diamond$, modified BEA; dashed line shows conventional BEA.

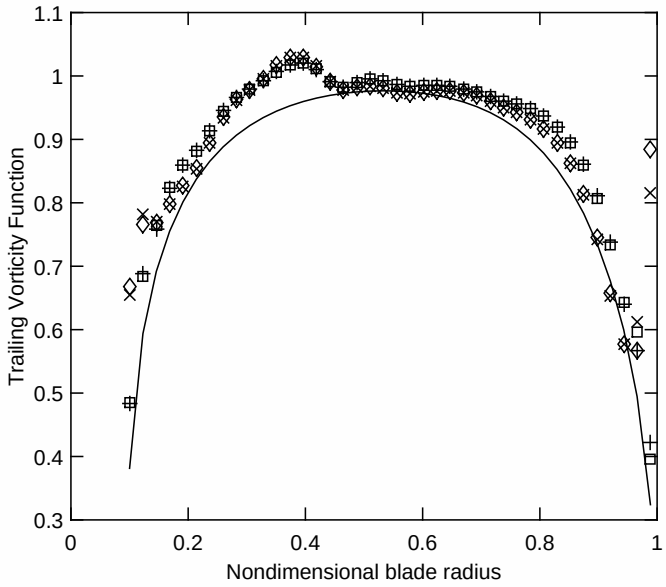

Figure 8: Calculated trailing vorticity functions for experiment of of Anderson et al. [23], $\lambda = 7$. $+$, F_u from Equation (8); $\square$,F_u from Equation (18); $\times$, F_w from Equation (9); $\Diamond$,F_w from Equation (18); solid line, F_P.

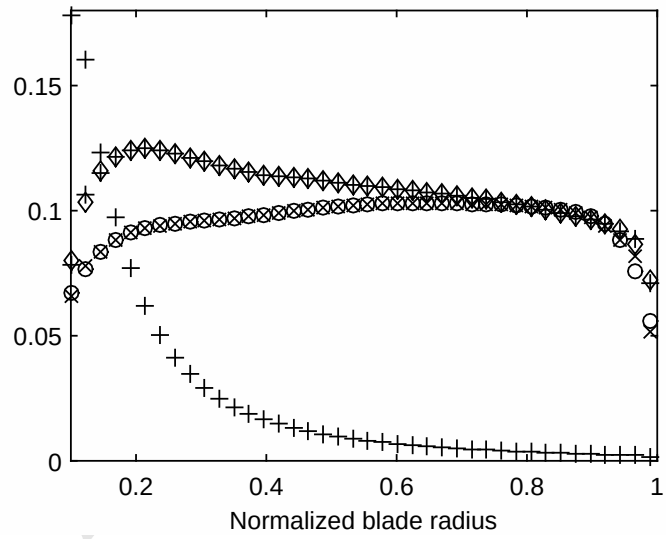

Figure 9: Modified BEA calculations of rotational induction, pitch and circulation for experiment of Anderson et al. [23], $\lambda = 7$. $+, a'F_w$; $\diamond$, Γ from Equation (21); $+$, Γ from Equation (19); $\circ$, p from Equation (21); $\times$, p from Equation (20).

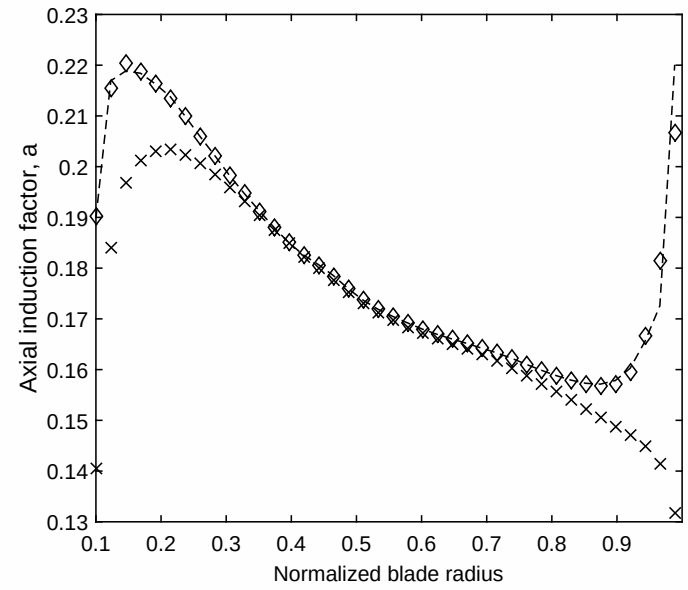

Figure 10: Calculated axial induction factor for experiment of of Anderson et al. [23], $\lambda = 7$. $\Diamond$, modified BEA, from Equation (**); dashed line, modified BEA from Equation (**); $\times$, conventional BEA

Highlights

- A new method of including finite blade numbers in blade element analysis is described.
- A numerical implementation of the new method is compared to wind tunnel experiments on model rotors.
- The new method gives improved performance by extracting more power near the blade tip.